A WEIGHTED LEAST-SQUARES FINITE ELEMENT METHOD FOR BIOT'S CONSOLIDATION PROBLEM

HSUEH-CHEN LEE AND HYESUK LEE

Abstract. This paper examines a weighted least-squares method for a poroelastic structure governed by Biot's consolidation model. Quasi-static model equations are converted to a first-order system of four-field, and the least-squares functional is defined for the time discretized system. We consider two different sets of weights for the functional and show its coercivity and continuity properties, from which an a priori error estimate for the primal variables is derived. Numerical experiments are provided to illustrate the performance of the proposed method.

Key words. Weighted least-squares finite element method, Biot's consolidation model.

1. Introduction

Biots consolidation model provides a general description of the mechanical behavior of a poroelastic medium and is frequently used in a wide range of applications in geomechanics, bioengineering, environmental engineering, and various other science and engineering areas. The model is based on the equation of linear elasticity for a solid matrix and Darcys law for the fluid flow through a porous matrix [2, 3]. Generally, solutions of the model are approximated by numerical methods since the analytical solution can only be derived under the assumption of special conditions [32, 36]. Finite element methods are commonly used in simulations. There have been various finite element methods proposed for the poroelasticity, including mixed finite element methods [15, 26, 28, 31, 35], discontinuous Galerkin finite element methods [13, 19], least-square methods [20, 21, 33], and hybrid methods [22, 29, 34] and a decoupling approach [14].

Problems for which solutions are smooth can be solved by standard finite element discretization. However, a finite element solution may have non-physical oscillations, known as pressure locking, if it displays some high-pressure gradient [15, 16, 17]. For example, pressure locking can occur when finite element spaces are not compatible. Some hybrid finite element methods [29, 35] have been proposed to overcome this issue. Another locking phenomenon called elasticity locking is observed when one of the Lamé coefficients becomes large, with the Poisson ratio approaching 0.5 [30].

The difficulties caused by the incompatibility of the spaces can be avoided by least-squares finite element methods. One of the main advantages of least-squares finite element methods is that no inf-sup condition is required between finite element spaces. Such flexibility makes the least-squares approach appealing for the finite element approximation of differential equations with multiple variables. This work aims to study a weighted least-squares (WLS) functional defined for the time discretized quasi-static Biot model and compares numerical solutions by the WLS finite element method with various weights. The WLS functional is defined using the L^2 -norm of the equation residuals multiplied by appropriately adjusted weights. Various developments have been reported for WLS finite element methods applied

to flow problems. Bochev and Gunzburger [4] developed a mesh-dependent weight of the WLS functional for Stokes flows based on the Agmon-Douglas-Nirenberg (ADN) approach. Weighted-norm least-squares methods were considered for problems with corner or coefficient singularities in [4], [40], [23]. In addition, Lee and Chen [24] applied a nonlinear weight to least-squares functional for Stokes equations, and this approach was further developed for non-Newtonian viscoelastic fluids [42], [25].

While extensive work on finite element approximations and analysis have been devoted to the Biot model, only a few studies of least-squares finite element methods have been carried out for the model [20, 21, 83]. In [20], Korsawe and Starke developed a four-field mixed least-squares finite element method for the quasi-static model with a simplified mass equation and unified modeling parameters. They defined the least-squares functional for the stationary case that arises at each time step to solve the temporal discretized model and proved the coercivity and continuity of the functional. In [21], Korsawe et al. numerically studied the Biot model and compared least-squares results with the standard Galerkin method results. The authors discussed the accuracy of stress and flux variables approximated directly in the least-squares method, pointing out that the additional unknowns increase the degree of freedom of the discretized problem compared to the Galerkin method. Tchonkova et al. discussed the mixed least-squares method for the poroelasticity problem of four-field and approximated solutions using linear continuous polynomials for all variables on triangle elements 33. However, in 21, 33, no weights were considered for the least-squares functionals.

This work further develops the least-squares approach and analysis presented in [20] for the full quasi-static model with all modeling parameters. We consider a WLS finite element method in a similar setting presented in [20]; the least-squares functional is defined for the four-field modeling equations discretized in time, where a weight for each term of the functional is appropriately chosen. Some of those weights need to be dependent on the time step for the analysis of the WLS functional. The choice of different sets of weights is also addressed. The WLS functional is then analyzed for the coercivity and continuity properties. It is demonstrated that the use of weights for the functional is helpful for the analysis and improves the accuracy of numerical solutions. Further, we extend the implementation to the intracranial pressure simulation [18].

The rest of this paper is organized as follows. Section presents the model equations and the least-square functional. Section introduces the WLS functional and the analysis for the functional. Section presents finite element spaces and error estimation of finite element approximations. Section provides two numerical examples, where numerical solutions by different sets of weights are compared, and finally, conclusions follow in Section .

2. Model equations and least-squares functional

Let Ω be a bounded, connected domain in \mathbb{R}^d , d=2,3 with the Lipschitz boundary $\partial\Omega$. Consider the quasi-static poroelastic system represented by the Biot model \square :

(1)
$$\nabla \cdot \mathbf{u} + \frac{\partial}{\partial t} (c_s p + \alpha \nabla \cdot \boldsymbol{\eta}) = f_s \text{ in } \Omega,$$

(2)
$$\mathbf{u} + K \nabla p = \mathbf{0} \text{ in } \Omega,$$

(2)
$$\mathbf{u} + K \nabla p = \mathbf{0} \text{ in } \Omega,$$
(3)
$$-2\mu \nabla \cdot \varepsilon(\boldsymbol{\eta}) - \lambda \nabla(\nabla \cdot \boldsymbol{\eta}) + \alpha \nabla p = \mathbf{f}_b \text{ in } \Omega,$$

where **u** denotes the fluid velocity, η denotes the displacement field, p is the pore pressure of the fluid and $\epsilon(\eta) := 0.5(\nabla \eta + \nabla \eta^T)$ is the standard strain rate tensor. The parameter c_s is the constrained specific storage coefficient, α is the BiotCWillis coefficient, and $K = \kappa/\mu_f$ is the hydraulic conductivity with κ being the permeability and μ_f being the fluid viscosity. In (2) μ and λ are the Lamé coefficients, which is computed by the Youngs modulus E and the Poisson ratio ν :

$$\mu = \frac{E \nu}{2(1+\nu)}, \quad \lambda = \frac{E \nu}{(1+\nu)(1-2\nu)}.$$

The right hand side functions f_s , \mathbf{f}_b are the source/sink term and the body force, respectively. The Biot system describes the fluid flow and elasticity of a saturated porous medium. In the model above, (III) is the storage equation for the mass conservation in the pores of the matrix, (Z) is Darcy's law, and (S) is the momentum equation for the balance of total forces. Let the boundary of domain, $\partial\Omega$ be decomposed into two pairs of disjoint sets such that $\partial \Omega = \Gamma_{pD} \cup \Gamma_{pN}$ and $\partial \Omega = \Gamma_{dD} \cup \Gamma_{dN}$. Assume that none of Γ_{pD} , Γ_{pN} , Γ_{dD} and Γ_{dN} has measure 0. The Biot model is completed with the boundary conditions and initial conditions:

(4)
$$p = 0$$
 on Γ_{pD} , $\mathbf{u} \cdot \mathbf{n} = 0$ on Γ_{pN} ,

(4)
$$p = 0$$
 on Γ_{pD} , $\mathbf{u} \cdot \mathbf{n} = 0$ on Γ_{pN} ,
(5) $\boldsymbol{\eta} = \mathbf{0}$ on Γ_{dD} , $\boldsymbol{\sigma} \cdot \mathbf{n} = \mathbf{0}$ on Γ_{dN} ,

(6)
$$p = p_0, \qquad \boldsymbol{\eta} = \boldsymbol{\eta}_0 \qquad \text{for } t = 0,$$

where we consider homogeneous boundary conditions for simplicity. However, the formulation of the least-squares functional and related analysis are extendable without additional technical or computational difficulties. In order to formulate the least-squares functional, we introduce the elastic stiffness tensor \mathcal{C} \square :

(7)
$$C\varepsilon(\boldsymbol{\eta}) = 2\mu\,\varepsilon(\boldsymbol{\eta}) + \lambda\,(tr\varepsilon(\boldsymbol{\eta}))\mathbf{I},$$

which can be regarded as a symmetric positive linear mapping. Let σ be the stress tensor from linear elasticity satisfying

(8)
$$\sigma = \mathcal{C}\varepsilon(\eta).$$

For finite element approximations of the linear elasticity with a large $\lambda > 0$ for nearly incompressible materials, the equation

(9)
$$C^{-1} \boldsymbol{\sigma} = \varepsilon(\boldsymbol{\eta})$$

is often considered instead of (8) for a locking-free formulation. Here, \mathcal{C}^{-1} is the compliance tensor given by [9, 26]

(10)
$$C^{-1}\boldsymbol{\sigma} = \frac{1}{2\mu}\boldsymbol{\sigma} - \frac{\lambda}{2\mu(d\lambda + 2\mu)}(tr\boldsymbol{\sigma})\mathbf{I},$$

where d is the dimension of Ω . Using $(\overline{\Omega})$, $(\underline{\aleph})$ and the backward Euler method, the time discretized first order system for (II)-(I) is written as

(11)
$$\nabla \cdot \mathbf{u} + \frac{1}{\Delta t} \left(c_s(p - p^{old}) + \alpha (\nabla \cdot \boldsymbol{\eta} - \nabla \cdot \boldsymbol{\eta}^{old}) \right) = f_s \text{ in } \Omega,$$

(12)
$$\mathbf{u} + K \nabla p = \mathbf{0} \text{ in } \Omega,$$

(13)
$$-\nabla \cdot (\boldsymbol{\sigma} - \alpha p \mathbf{I}) = \mathbf{f}_b \text{ in } \Omega,$$

(14)
$$\boldsymbol{\sigma} - \mathcal{C}\varepsilon(\boldsymbol{\eta}) = \mathbf{0} \text{ in } \Omega,$$

where Δt is the fixed time step size and p^{old} , η^{old} denote the pressure and displacement fields at the previous time-step, respectively.

Let $H^s\left(\Omega\right),\ s\geq 0$, be the Sobolev spaces with the standard associated inner products $(\cdot,\cdot)_s$ and their respective norms $\|\cdot\|_s$. For $s=0,\ H^s(\Omega)$ coincides with $L^2\left(\Omega\right)$ and we use $\|\cdot\|$ for $\|\cdot\|_0$. Let $H_{div}(\Omega)=\{v\in L^2(\Omega):\nabla\cdot v\in L^2(\Omega)\}$ be the Hilbert space equipped with the norm $\|v\|_{H_{div}(\Omega)}=(\|v\|^2+\|\nabla\cdot v\|^2)^{1/2}$. The corresponding space of vector-valued or tensor-valued functions is written in boldface.

To consider the least-squares functional, we first introduce the function spaces for $(\sigma, \eta, \mathbf{u}, p)$:

$$\mathbf{S} := \{ \boldsymbol{\tau} \in \mathbf{H}_{div}(\Omega) : \tau_{ij} = \tau_{ji}, \ 1 \leq i, j \leq d, \ \boldsymbol{\tau} \cdot \mathbf{n} = \mathbf{0} \text{ on } \Gamma_{dN} \},$$

$$\Sigma := \{ \boldsymbol{\xi} \in \mathbf{H}^1(\Omega) : \boldsymbol{\xi} = \mathbf{0} \text{ on } \Gamma_{dD} \},$$

$$\mathbf{X} := \{ \mathbf{v} \in \mathbf{H}_{div}(\Omega) : \mathbf{v} \cdot \mathbf{n} = 0 \text{ on } \Gamma_{pN} \},$$

$$Q := \{ q \in H^1(\Omega) : q = 0 \text{ on } \Gamma_{pD} \},$$

and define the product space $\Phi = \mathbf{S} \times \mathbf{\Sigma} \times \mathbf{X} \times Q$. The standard least-squares functional for ([11])-([14]) is then defined by

(15)
$$\mathcal{L}(\boldsymbol{\sigma}, \ \boldsymbol{\eta}, \ \mathbf{u}, \ p; \ \mathbf{F}) := \|\nabla \cdot \mathbf{u} + \frac{1}{\Delta t} \left(c_s p + \alpha \nabla \cdot \boldsymbol{\eta}\right) - \hat{f}\|^2 + \|\nabla \cdot (\boldsymbol{\sigma} - \alpha p \mathbf{I}) + \mathbf{f}_b\|^2 + \|\mathbf{u} + K \nabla p\|^2 + \|\boldsymbol{\sigma} - C\varepsilon(\boldsymbol{\eta})\|^2,$$

where
$$\hat{f} := f_s + \frac{1}{\Delta t} \left(\alpha \nabla \cdot \boldsymbol{\eta}^{\text{old}} + c_s p^{\text{old}} \right)$$
 and $\mathbf{F} := (\hat{f}, \mathbf{f}_b)$.

In this work we consider a scaled stress equation instead of (\square) for the proper balance of terms in the WLS functional to be introduced. Being scaled by $\mathcal{C}^{-1/2}$, (\square 4) can be written in the alternate locking-free formulation for nearly incompressible materials \square 7, \square 8, \square 9:

(16)
$$\mathcal{C}^{-1/2} \boldsymbol{\sigma} - \mathcal{C}^{1/2} \varepsilon(\boldsymbol{\eta}) = \mathbf{0},$$

where, for $\tau \in \mathbf{S}$, $C^{1/2}\tau$ and $C^{-1/2}\tau$ are given by

(17)
$$\mathcal{C}^{1/2}\boldsymbol{\tau} = \sqrt{2\mu}\,\boldsymbol{\tau} + \frac{-\sqrt{2\mu} + \sqrt{2\mu + d\lambda}}{d}(tr\boldsymbol{\tau})I,$$

(18)
$$\mathcal{C}^{-1/2} \boldsymbol{\tau} = \frac{1}{\sqrt{2\mu}} \boldsymbol{\tau} + \frac{1}{d} \left(-\frac{1}{\sqrt{2\mu}} + \frac{1}{\sqrt{d\lambda + 2\mu}} \right) (tr \boldsymbol{\tau}) I,$$

respectively. The identity in (1721) can be easily derived based on

(19)
$$\|\mathcal{C}^{1/2}\boldsymbol{\tau}\|^2 = (\mathcal{C}\boldsymbol{\tau}, \boldsymbol{\tau}) = 2\mu\|\boldsymbol{\tau}\|^2 + \lambda((tr\,\boldsymbol{\tau})I, \boldsymbol{\tau}) = 2\mu\|\boldsymbol{\tau}\|^2 + \lambda\|tr\,\boldsymbol{\tau}\|^2.$$

Similarly, using (\square) , we see that

(20)
$$\|\mathcal{C}^{-1/2}\boldsymbol{\tau}\|^2 = (\mathcal{C}^{-1}\boldsymbol{\tau},\boldsymbol{\tau}) = \frac{1}{2\mu}\|\boldsymbol{\tau}\|^2 - \frac{\lambda}{2\mu(d\boldsymbol{\tau} + 2\mu)}\|tr\,\boldsymbol{\tau}\|^2,$$

from which (18) is obtained.

We now define the WLS functional for (11)-(13) and (16):

$$\mathcal{J}(\boldsymbol{\sigma}, \boldsymbol{\eta}, \mathbf{u}, p; \mathbf{F}) := W_1 \|\nabla \cdot \mathbf{u} + \frac{1}{\Delta t} (c_s p + \alpha \nabla \cdot \boldsymbol{\eta}) - \hat{f}\|^2$$

$$(21) \qquad +W_2\|\nabla\cdot(\boldsymbol{\sigma}-\alpha p\mathbf{I})+\mathbf{f}_b\|^2+W_3\|\mathbf{u}+K\nabla p\|^2+W_4\|\mathcal{C}^{-1/2}\boldsymbol{\sigma}-\mathcal{C}^{1/2}\varepsilon(\boldsymbol{\eta})\|^2,$$

where W_i for i=1,2,3,4 are positive constants. Some of those weights will be chosen in terms of the time step as in [III], [ZII]. Consider ([ZII]) with the choice of $(W_1, W_2, W_3, W_4) = (\Delta t, 1, \Delta t, 1)$:

$$\mathcal{J}_{\Delta t}^{1}(\boldsymbol{\sigma}, \boldsymbol{\eta}, \mathbf{u}, p; \mathbf{F}) := \Delta t \|\nabla \cdot \mathbf{u} + \frac{1}{\Delta t} \left(c_{s} p + \alpha \nabla \cdot \boldsymbol{\eta}\right) - \hat{f}\|^{2}$$

(22)
$$+\|\nabla \cdot (\boldsymbol{\sigma} - \alpha p \mathbf{I}) + \mathbf{f}_b\|^2 + \Delta t \|\mathbf{u} + K \nabla p\|^2 + \|\mathcal{C}^{-1/2} \boldsymbol{\sigma} - \mathcal{C}^{1/2} \varepsilon(\boldsymbol{\eta})\|^2.$$

The corresponding homogeneous functional of $\mathcal{J}_{\Delta t}^1$ was analyzed in [20] for the reduced model with $c_s=0$ and $\alpha=K=1$. We also consider (21) with $(W_1,W_2,W_3,W_4)=(1,1,\Delta t,1)$:

$$\mathcal{J}_{\Delta t}^{2}(\boldsymbol{\sigma}, \boldsymbol{\eta}, \mathbf{u}, p; \mathbf{F}) := \|\nabla \cdot \mathbf{u} + \frac{1}{\Delta t} \left(c_{s} p + \alpha \nabla \cdot \boldsymbol{\eta}\right) - \hat{f}\|^{2}$$

$$+ \|\nabla \cdot (\boldsymbol{\sigma} - \alpha p \mathbf{I}) + \mathbf{f}_{b}\|^{2} + \Delta t \|\mathbf{u} + K \nabla p\|^{2} + \|\mathcal{C}^{-1/2} \boldsymbol{\sigma} - \mathcal{C}^{1/2} \varepsilon(\boldsymbol{\eta})\|^{2}.$$

3. Analysis of LS functional

In this section we will show that the homogeneous functionals of $\mathcal{J}_{\Delta t}^{i}$ for i=1,2 are coercive and continuous. For the analysis purpose, we assume that $\Delta t \leq 1$ throughout this paper without loss of generality. First, we introduce new variables needed for the analysis. Let

(24)
$$\tilde{\boldsymbol{\sigma}} := \boldsymbol{\sigma} - \alpha p \mathbf{I}, \qquad \tilde{\mathbf{u}} := \mathbf{u} + \alpha \frac{1}{\Delta t} \boldsymbol{\eta}.$$

To determine appropriate function spaces for the new variables, assume that $\Gamma_{pD} = \Gamma_{dN} =: \Gamma_a$ and $\Gamma_{dD} = \Gamma_{pN} =: \Gamma_b$, which allows $\tilde{\boldsymbol{\sigma}}$, $\tilde{\mathbf{u}}$ to be in \mathbf{S} and \mathbf{X} , respectively. Define the scaled norm

$$\|(\boldsymbol{\tau}, \boldsymbol{\xi}, \mathbf{v}, q)\|_{\Delta t}^{2} = \|\nabla \cdot \boldsymbol{\tau}\|^{2} + \|\mathcal{C}^{-1/2}\boldsymbol{\tau}\|^{2} + \|\mathcal{C}^{1/2}\epsilon(\boldsymbol{\xi})\|^{2}$$

$$+ (\Delta t)^{2} \|\nabla \cdot \mathbf{v}\|^{2} + \Delta t \|\mathbf{v}\|^{2} + \Delta t \|\nabla q\|^{2} + \|q\|^{2}$$

$$(25)$$

for all $(\tau, \xi, \mathbf{v}, q) \in \Phi$. In the analyses followed, we will use Korn's inequality for the scaled strain tensor:

(26)
$$\|\boldsymbol{\xi}\|^2 + \|\nabla \boldsymbol{\xi}\|^2 \le C_K \|\mathcal{C}^{1/2} \varepsilon(\boldsymbol{\xi})\|^2.$$

In the following Lemma we show that the scaled norm of new variables is equivalent to the scaled norm of the original unknown variables.

Lemma 3.1. There is a constant $\overline{C} > 0$ such that

(27)
$$\frac{1}{\overline{C}} \|(\boldsymbol{\tau}, \boldsymbol{\xi}, \mathbf{v}, q)\|_{\Delta t}^2 \le \|(\tilde{\boldsymbol{\tau}}, \boldsymbol{\xi}, \tilde{\mathbf{v}}, q)\|_{\Delta t}^2 \le \overline{C} \|(\boldsymbol{\tau}, \boldsymbol{\xi}, \mathbf{v}, q)\|_{\Delta t}^2,$$

for all $(\tau, \xi, \mathbf{v}, q)$, $(\tilde{\tau}, \xi, \tilde{\mathbf{v}}, q) \in \mathbf{\Phi}$.

Proof. Using $(a+b)^2 \leq 2(a^2+b^2)$, we can have $\|(\boldsymbol{\tau},\boldsymbol{\xi},\mathbf{v},q)\|_{\Delta t}^2$ bounded as

$$\begin{split} \|(\boldsymbol{\tau}, \boldsymbol{\xi}, \mathbf{v}, q)\|_{\Delta t}^{2} &= \|(\tilde{\boldsymbol{\tau}} + \alpha q \mathbf{I}, \boldsymbol{\xi}, \tilde{\mathbf{v}} - \frac{\alpha}{\Delta t} \boldsymbol{\xi}, q)\|_{\Delta t}^{2} \\ &= \|\nabla \cdot (\tilde{\boldsymbol{\tau}} + \alpha q \mathbf{I})\|^{2} + \|\mathcal{C}^{-1/2}(\tilde{\boldsymbol{\tau}} + \alpha q \mathbf{I})\|^{2} + \|\mathcal{C}^{1/2} \epsilon(\boldsymbol{\xi})\|^{2} \\ &+ (\Delta t)^{2} \|\nabla \cdot (\tilde{\mathbf{v}} + \frac{\alpha}{\Delta t} \boldsymbol{\xi})\|^{2} + \Delta t \|\tilde{\mathbf{v}} + \frac{\alpha}{\Delta t} \boldsymbol{\xi}\|^{2} + \Delta t \|\nabla q\|^{2} + \|q\|^{2} \\ &\leq 2 \|\nabla \cdot \tilde{\boldsymbol{\tau}}\|^{2} + 2 \|\mathcal{C}^{-1/2} \tilde{\boldsymbol{\tau}}\|^{2} + \|\mathcal{C}^{1/2} \epsilon(\boldsymbol{\xi})\|^{2} + 2\alpha^{2} \|\nabla \cdot \boldsymbol{\xi}\|^{2} + \frac{2\alpha^{2}}{\Delta t} \|\boldsymbol{\xi}\|^{2} \\ &+ 2(\Delta t)^{2} \|\nabla \cdot \tilde{\mathbf{v}}\|^{2} + 2\Delta t \|\tilde{\mathbf{v}}\|^{2} \\ &+ (2\alpha^{2} + \Delta t) \|\nabla q\|^{2} + \|q\|^{2} + 2\alpha^{2} \|\mathcal{C}^{-1/2}(q \mathbf{I})\|^{2}. \end{split}$$

Poincaré-Friedrichs inequality and C^{-1} in (\square) yield

(28)
$$\|\mathcal{C}^{-1/2}(q\mathbf{I})\|^2 = (q\mathbf{I}, \mathcal{C}^{-1}(q\mathbf{I})) = \frac{d}{d\lambda + 2u}\|q\|^2 \le \frac{dC_{PF}^2}{d\lambda + 2u}\|\nabla q\|^2.$$

Therefore, by (26),

$$\|(\boldsymbol{\tau}, \boldsymbol{\xi}, \mathbf{v}, q)\|_{\Delta t}^{2} \leq 2(\|\nabla \cdot \tilde{\boldsymbol{\tau}}\|^{2} + \|\mathcal{C}^{-1/2}\tilde{\boldsymbol{\tau}}\|^{2}) + \left(1 + \frac{4\alpha^{2}C_{K}}{\Delta t}\right)\|\mathcal{C}^{1/2}\epsilon(\boldsymbol{\xi})\|^{2} + 2(\Delta t)^{2}\|\nabla \cdot \tilde{\mathbf{v}}\|^{2} + 2\Delta t\|\tilde{\mathbf{v}}\|^{2} + \left(1 + \frac{2\alpha^{2}}{\Delta t} + \frac{2\alpha^{2}dC_{PF}^{2}}{\Delta t(d\lambda + 2\mu)}\right)\Delta t\|\nabla q\|^{2} + \|q\|^{2},$$
(29)

where C_K , C_{PF} are constants for Korn's and Poincaré-Friedrichs inequalities, respectively. If we choose $\overline{C} = max \left\{ 2, 1 + \frac{4\alpha^2 C_K}{\Delta t}, 1 + \frac{2\alpha^2}{\Delta t} + \frac{2\alpha^2 d \, C_{PF}^2}{\Delta t (d\lambda + 2\mu)} \right\}$, the first inequality in (ZZ) follows from (ZZ). As $\|(\tilde{\tau}, \boldsymbol{\xi}, \tilde{\mathbf{v}}, q)\|_{\Delta t}^2 = \|(\boldsymbol{\tau} - \alpha q \mathbf{I}, \boldsymbol{\xi}, \mathbf{v} + \frac{\alpha}{\Delta t} \boldsymbol{\xi}, q)\|_{\Delta t}^2$, the second inequality is also obtained by the same argument.

Remark 3.1. To analyze the WLS functionals (22) and (23), the divergence term $\|\nabla \cdot \mathbf{v}\|$ in (25) needs to be scaled by $(\Delta t)^2$, unlike the scaled norm introduced for the Biot model with $c_s = 0$ in [20].

Korsawe and Starke [20] derived coercivity and continuity estimates for the homogeneous functional of (22) with $c_s = 0$ and established the a priori estimate. In this work, we analyze (22) and (23) for the full quasi-static Biot model with a nonzero storage coefficient, i.e., $c_s \neq 0$.

Theorem 3.1. For all $(\sigma, \eta, \mathbf{u}, p)$, $(\tilde{\sigma}, \eta, \tilde{\mathbf{u}}, p) \in \Phi$ and i = 1, 2, there are positive constants C_1 , C_2 satisfying

(30)
$$C_1 \| (\tilde{\boldsymbol{\sigma}}, \boldsymbol{\eta}, \tilde{\mathbf{u}}, p) \|_{\Delta t}^2 \le J_{\Delta t}^i(\boldsymbol{\sigma}, \boldsymbol{\eta}, \mathbf{u}, p; \mathbf{0}) \le C_2 \| (\tilde{\boldsymbol{\sigma}}, \boldsymbol{\eta}, \tilde{\mathbf{u}}, p) \|_{\Delta t}^2,$$

where C_1 is independent of the time step Δt , while C_2 depends on Δt .

Proof. We will first consider $J_{\Delta t}^1(\sigma, \eta, \mathbf{u}, p; \mathbf{0})$ and show its lower bound. Let M, A and B be positive constants to be specified later. The functional (22) is bounded in terms of the variables defined in (24) as

$$\begin{aligned} & \max\{M,A,K+B\} \, J_{\Delta t}^{1}(\boldsymbol{\sigma},\boldsymbol{\eta},\mathbf{u},p;\mathbf{0}) \\ &= \max\{M,A,K+B\} \, J_{\Delta t}(\tilde{\boldsymbol{\sigma}}+\alpha\,p\mathbf{I},\boldsymbol{\eta},\tilde{\mathbf{u}}-\alpha\frac{1}{\Delta t}\boldsymbol{\eta},p;\mathbf{0}) \\ &\geq M\,\Delta t\, \|\nabla\cdot\tilde{\mathbf{u}}+\frac{c_{s}}{\Delta t}p\|^{2}+A\|\nabla\cdot\tilde{\boldsymbol{\sigma}}\|^{2} \\ &+\Delta t\, \|\tilde{\mathbf{u}}+K\,\nabla p-\frac{\alpha}{\Delta t}\boldsymbol{\eta}\|^{2}+(K+B)\|\mathcal{C}^{-1/2}(\tilde{\boldsymbol{\sigma}}+\alpha p\mathbf{I})-\mathcal{C}^{1/2}\varepsilon(\boldsymbol{\eta})\|^{2} \\ &= M\Delta t\, \|\nabla\cdot\tilde{\mathbf{u}}+\frac{c_{s}}{\Delta t}p\|^{2}+A\|\nabla\cdot\tilde{\boldsymbol{\sigma}}\|^{2}+\Delta t\, \|\tilde{\mathbf{u}}+K\,\nabla p\|_{0}^{2}+\frac{\alpha^{2}}{\Delta t}\|\boldsymbol{\eta}\|^{2} \\ &+B\|\mathcal{C}^{-1/2}(\tilde{\boldsymbol{\sigma}}+\alpha p\mathbf{I})-\mathcal{C}^{1/2}\varepsilon(\boldsymbol{\eta})\|^{2}+K\, \|\mathcal{C}^{-1/2}\tilde{\boldsymbol{\sigma}}-\mathcal{C}^{1/2}\varepsilon(\boldsymbol{\eta})\|^{2} \\ &+\alpha^{2}K\, \|\mathcal{C}^{-1/2}(p\mathbf{I})\|^{2}+2\alpha K\, (tr(\mathcal{C}^{-1}\tilde{\boldsymbol{\sigma}})-\nabla\cdot\boldsymbol{\eta},p)-2\alpha(\tilde{\mathbf{u}}+K\nabla p,\boldsymbol{\eta}), \end{aligned}$$

where the second equality follows from the identity

$$(\mathcal{C}^{-1/2}\tilde{\boldsymbol{\sigma}} - \mathcal{C}^{1/2}\varepsilon(\boldsymbol{\eta}), \, \mathcal{C}^{-1/2}(p\mathbf{I})) = (\mathcal{C}^{-1}\tilde{\boldsymbol{\sigma}} - \varepsilon(\boldsymbol{\eta}), \, p\mathbf{I}) = (tr(\mathcal{C}^{-1}\tilde{\boldsymbol{\sigma}}) - \nabla \cdot \boldsymbol{\eta}, \, p).$$

Next, we use the result from Lemma 4.2 in [20]:

(31)
$$||as \,\tilde{\sigma}||^2 \le 2\mu \, ||\mathcal{C}^{-1/2}(\tilde{\sigma} + \alpha p\mathbf{I}) - \mathcal{C}^{1/2}\varepsilon(\boldsymbol{\eta})||^2$$

where $as \,\tilde{\boldsymbol{\sigma}}$ is the antisymmetric part of $\tilde{\boldsymbol{\sigma}}$ define by $as \,\tilde{\boldsymbol{\sigma}} = (\tilde{\boldsymbol{\sigma}} - \tilde{\boldsymbol{\sigma}}^T)/2$. In [20], was proved for $\alpha = 1$. However, since the diagonal elements of $as \,\tilde{\boldsymbol{\sigma}}$ are zero,

the estimate holds for any α . Now, using (BII), (III), (ZN), we have

$$\max\{M, A, K + B\} J_{\Delta t}^{1}(\boldsymbol{\sigma}, \boldsymbol{\eta}, \mathbf{u}, p; \mathbf{0})$$

$$\geq M \Delta t \|\nabla \cdot \tilde{\mathbf{u}} + \frac{c_{s}}{\Delta t}p\|^{2} + A\|\nabla \cdot \tilde{\boldsymbol{\sigma}}\|^{2} + \Delta t \|\tilde{\mathbf{u}} + K \nabla p\|^{2} + \frac{\alpha^{2}}{\Delta t} \|\boldsymbol{\eta}\|^{2}$$

$$+ \frac{B}{2\mu} \|as \, \tilde{\boldsymbol{\sigma}}\|^{2} + K \|\mathcal{C}^{-1/2} \tilde{\boldsymbol{\sigma}} - \mathcal{C}^{1/2} \varepsilon(\boldsymbol{\eta})\|^{2}$$

$$+ \frac{\alpha^{2}Kd}{d\lambda + 2\mu} \|p\|^{2} + 2\alpha K \left(\frac{1}{d\lambda + 2\mu} tr \, \tilde{\boldsymbol{\sigma}}, p\right) - 2\alpha(\tilde{\mathbf{u}}, \boldsymbol{\eta}).$$
(32)

By Young's inequality the last two terms in (22) are bounded as

$$2\alpha K \left(\frac{1}{d\lambda + 2\mu} tr \, \tilde{\boldsymbol{\sigma}}, p \right) \geq -\frac{\epsilon_1}{d(d\lambda + 2\mu)} \|tr \, \tilde{\boldsymbol{\sigma}}\|^2 - \frac{\alpha^2 K^2 d}{\epsilon_1 (d\lambda + 2\mu)} \|p\|^2,$$
$$-2\alpha (\tilde{\mathbf{u}}, \boldsymbol{\eta}) \geq -\frac{\alpha^2}{\epsilon_2 \Delta t} \|\boldsymbol{\eta}\|^2 - \epsilon_2 \Delta t \|\tilde{\mathbf{u}}\|^2$$

for $\epsilon_1, \epsilon_2 > 0$. Thus, we have

$$\max\{M, A, K + B\}J_{\Delta t}^{1}(\boldsymbol{\sigma}, \boldsymbol{\eta}, \mathbf{u}, p; \mathbf{0})$$

$$\geq \left[A\|\nabla \cdot \tilde{\boldsymbol{\sigma}}\|^{2} + \frac{B}{2\mu}\|as\,\tilde{\boldsymbol{\sigma}}\|^{2} + K\|\mathcal{C}^{-1/2}\tilde{\boldsymbol{\sigma}} - \mathcal{C}^{1/2}\varepsilon(\boldsymbol{\eta})\|^{2}\right]$$

$$-\frac{\epsilon_{1}}{d(d\lambda + 2\mu)}\|tr\,\tilde{\boldsymbol{\sigma}}\|^{2} + \frac{\alpha^{2}}{\Delta t}\left(1 - \frac{1}{\epsilon_{2}}\right)\|\boldsymbol{\eta}\|^{2}\right]$$

$$+ \left[M\,\Delta t\,\|\nabla \cdot \tilde{\mathbf{u}} + \frac{c_{s}}{\Delta t}p\|^{2} + \Delta t\,\|\tilde{\mathbf{u}} + K\nabla p\|^{2} - \epsilon_{2}\,\Delta t\,\|\tilde{\mathbf{u}}\|^{2}\right]$$

$$-\alpha^{2}d\left(\frac{K^{2}}{\epsilon_{1}} - K\right)\frac{1}{d\lambda + 2\mu}\|p\|^{2}$$

$$:= \mathcal{L}_{1}(\tilde{\boldsymbol{\sigma}}, \boldsymbol{\eta}) + \mathcal{L}_{2}(\tilde{\mathbf{u}}, p).$$

The $\mathcal{L}_1(\tilde{\boldsymbol{\sigma}}, \boldsymbol{\eta})$ term is similar to the corresponding term in [20] (see p329) and estimated by a similar way, however, $\mathcal{L}_2(\tilde{\boldsymbol{\sigma}}, \boldsymbol{\eta})$ includes an additional term that requires special care.

We first consider $\mathcal{L}_1(\tilde{\boldsymbol{\sigma}}, \boldsymbol{\eta})$. Note that $\|\tilde{\boldsymbol{\sigma}}\|^2 \geq \frac{1}{d} \|tr\,\tilde{\boldsymbol{\sigma}}\|^2$ by Young's inequality. Thus,

$$\begin{split} \|\mathcal{C}^{-1/2}\tilde{\boldsymbol{\sigma}}\|^2 &= (\mathcal{C}^{-1}\tilde{\boldsymbol{\sigma}},\,\tilde{\boldsymbol{\sigma}}) = \frac{1}{2\mu}\|\tilde{\boldsymbol{\sigma}}\|^2 - \frac{\lambda}{2\mu(d\lambda + 2\mu)}\|tr\,\tilde{\boldsymbol{\sigma}}\|^2 \\ &= \frac{1}{2\mu}(\|\tilde{\boldsymbol{\sigma}}\|^2 - \frac{1}{d}\|tr\,\tilde{\boldsymbol{\sigma}}\|^2) + \frac{1}{d(d\lambda + 2\mu)}\|tr\,\tilde{\boldsymbol{\sigma}}\|^2 \geq \frac{1}{d(d\lambda + 2\mu)}\|tr\,\tilde{\boldsymbol{\sigma}}\|^2, \end{split}$$

which implies

$$-\frac{\epsilon_1}{d(d\lambda + 2\mu)} \|tr\,\tilde{\boldsymbol{\sigma}}\|^2 \ge -\epsilon_1 \|\mathcal{C}^{-1/2}\tilde{\boldsymbol{\sigma}}\|^2.$$

Using this estimate and (26), and assuming $\epsilon_2 < 1$, we obtain

$$\mathcal{L}_{1}(\tilde{\boldsymbol{\sigma}}, \boldsymbol{\eta}) \geq A \|\nabla \cdot \tilde{\boldsymbol{\sigma}}\|^{2} + \frac{B}{2\mu} \|as \, \tilde{\boldsymbol{\sigma}}\|^{2} + K \|\mathcal{C}^{-1/2} \tilde{\boldsymbol{\sigma}} - \mathcal{C}^{1/2} \varepsilon(\boldsymbol{\eta})\|^{2} - \epsilon_{1} \|\mathcal{C}^{-1/2} \tilde{\boldsymbol{\sigma}}\|^{2}$$

$$+ \frac{\alpha^{2} C_{K}}{\Delta t} \left(1 - \frac{1}{\epsilon_{2}}\right) \|\mathcal{C}^{1/2} \varepsilon(\boldsymbol{\eta})\|^{2}$$

$$\geq A \|\nabla \cdot \tilde{\boldsymbol{\sigma}}\|^{2} + \frac{B}{2\mu} \|as \, \tilde{\boldsymbol{\sigma}}\|^{2} + (K - \epsilon_{1}) \|\mathcal{C}^{-1/2} \tilde{\boldsymbol{\sigma}}\|^{2}$$

$$-2K(\tilde{\boldsymbol{\sigma}}, \varepsilon(\boldsymbol{\eta})) + \left(K - \frac{\alpha^{2} C_{K}}{\Delta t} \left(\frac{1}{\epsilon_{2}} - 1\right)\right) \|\mathcal{C}^{1/2} \varepsilon(\boldsymbol{\eta})\|^{2}.$$

As $(as \,\tilde{\boldsymbol{\sigma}}, \varepsilon(\boldsymbol{\eta})) = 0$ and $\tilde{\boldsymbol{\sigma}} - as \,\tilde{\boldsymbol{\sigma}}$ is symmetric,

$$(\tilde{\boldsymbol{\sigma}}, \varepsilon(\boldsymbol{\eta})) = (\tilde{\boldsymbol{\sigma}} - as \, \tilde{\boldsymbol{\sigma}}, \varepsilon(\boldsymbol{\eta})) = (\tilde{\boldsymbol{\sigma}} - as \, \tilde{\boldsymbol{\sigma}}, \nabla \boldsymbol{\eta}) = -(\nabla \cdot \tilde{\boldsymbol{\sigma}}, \boldsymbol{\eta}) - (as \, \tilde{\boldsymbol{\sigma}}, \nabla \boldsymbol{\eta}).$$

Therefore, Young's and Korn's inequalities and the identity $a^2 + 2ab = (a+b)^2 - b^2$ yield

$$\mathcal{L}_{1}(\tilde{\boldsymbol{\sigma}}, \boldsymbol{\eta}) \geq A\|\nabla \cdot \tilde{\boldsymbol{\sigma}}\|^{2} + \frac{B}{2\mu}\|as\,\tilde{\boldsymbol{\sigma}}\|^{2} + (K - \epsilon_{1})\|\mathcal{C}^{-1/2}\tilde{\boldsymbol{\sigma}}\|^{2} + 2K(\nabla \cdot \tilde{\boldsymbol{\sigma}}, \boldsymbol{\eta})$$

$$+2K(as\,\tilde{\boldsymbol{\sigma}}, \nabla\boldsymbol{\eta}) + \left(K - \frac{\alpha^{2}C_{K}}{\Delta t}\left(\frac{1}{\epsilon_{2}} - 1\right)\right)\|\mathcal{C}^{1/2}\varepsilon(\boldsymbol{\eta})\|^{2}$$

$$\geq \left(A - \frac{1}{\epsilon_{3}}\right)\|\nabla \cdot \tilde{\boldsymbol{\sigma}}\|^{2} + (K - \epsilon_{1})\|\mathcal{C}^{-1/2}\tilde{\boldsymbol{\sigma}}\|^{2}$$

$$+ \left(K - \frac{\alpha^{2}C_{K}}{\Delta t}\left(\frac{1}{\epsilon_{2}} - 1\right)\right)\|\mathcal{C}^{1/2}\varepsilon(\boldsymbol{\eta})\|^{2} - K^{2}\epsilon_{3}\|\boldsymbol{\eta}\|^{2}$$

$$+ \|\left(\frac{B}{2\mu}\right)^{1/2}as\,\tilde{\boldsymbol{\sigma}} + K\left(\frac{2\mu}{B}\right)^{1/2}\nabla\boldsymbol{\eta}\|^{2} - K^{2}\frac{2\mu}{B}\|\nabla\boldsymbol{\eta}\|^{2}$$

$$\geq \left(A - \frac{1}{\epsilon_{3}}\right)\|\nabla \cdot \tilde{\boldsymbol{\sigma}}\|^{2} + (K - \epsilon_{1})\|\mathcal{C}^{-1/2}\tilde{\boldsymbol{\sigma}}\|^{2}$$

$$(33) + \left(K - \frac{\alpha^{2}C_{K}}{\Delta t}\left(\frac{1}{\epsilon_{2}} - 1\right) - C_{K}K^{2}\max\left\{\epsilon_{3}, \frac{2\mu}{B}\right\}\right)\|\mathcal{C}^{1/2}\varepsilon(\boldsymbol{\eta})\|^{2}$$

for some $\epsilon_3 > 0$. Therefore, by choosing $\epsilon_2 = \frac{1}{1 + \frac{\Delta t \, K}{4\alpha^2 C_K}}$, $\epsilon_3 = \frac{1}{4KC_K}$, $A = 8KC_K$, $B = \frac{2\mu}{\epsilon_3} = 8\mu KC_K$, the estimate for $\mathcal{L}_1(\tilde{\boldsymbol{\sigma}}, \boldsymbol{\eta})$ is obtained:

$$(34) \quad \mathcal{L}_1(\tilde{\boldsymbol{\sigma}}, \boldsymbol{\eta}) \quad \geq \quad 4KC_K \|\nabla \cdot \tilde{\boldsymbol{\sigma}}\|^2 + (K - \epsilon_1) \|\mathcal{C}^{-1/2} \tilde{\boldsymbol{\sigma}}\|^2 + \frac{K}{2} \|\mathcal{C}^{1/2} \varepsilon(\boldsymbol{\eta})\|^2.$$

Note that ϵ_1 in (34) should be less than K to ensure that the right hand side is positive.

Now we estimate $\mathcal{L}_2(\tilde{\mathbf{u}}, p)$. Using Poincaré-Friedrichs inequality and Young's inequality, the $\mathcal{L}_2(\tilde{\mathbf{u}}, p)$ term is bounded as

$$\mathcal{L}_{2}(\tilde{\mathbf{u}}, p) = M \Delta t \|\nabla \cdot \tilde{\mathbf{u}} + \frac{c_{s}}{\Delta t}p\|^{2} + \Delta t \|\tilde{\mathbf{u}} + K\nabla p\|^{2} - \epsilon_{2}\Delta t \|\tilde{\mathbf{u}}\|^{2}$$

$$-\alpha^{2}d\left(\frac{K^{2}}{\epsilon_{1}} - K\right) \frac{1}{d\lambda + 2\mu} \|p\|^{2}$$

$$\geq M \Delta t \|\nabla \cdot \tilde{\mathbf{u}}\|^{2} + M \frac{c_{s}^{2}}{\Delta t} \|p\|^{2} + 2Mc_{s}(\nabla \cdot \tilde{\mathbf{u}}, p) + \Delta t(1 - \epsilon_{2}) \|\tilde{\mathbf{u}}\|^{2}$$

$$+\Delta t K^{2} \|\nabla p\|^{2} + 2\Delta t K(\tilde{\mathbf{u}}, \nabla p) - \alpha^{2}d C_{PF}^{2} \left(\frac{K^{2}}{\epsilon_{1}} - K\right) \frac{1}{d\lambda + 2\mu} \|\nabla p\|^{2}$$

$$\geq M \Delta t \|\nabla \cdot \tilde{\mathbf{u}}\|^{2} + M \frac{c_{s}^{2}}{\Delta t} \|p\|^{2} + \Delta t(1 - \epsilon_{2}) \|\tilde{\mathbf{u}}\|^{2} + 2(Mc_{s} - \Delta t K)(\nabla \cdot \tilde{\mathbf{u}}, p)$$

$$(35) + \left(\Delta t K^{2} - \alpha^{2}d C_{PF}^{2} \left(\frac{K^{2}}{\epsilon_{1}} - K\right) \frac{1}{d\lambda + 2\mu}\right) \|\nabla p\|^{2}.$$

If M is a constant satisfying $M > \frac{\Delta t K}{c_s}$, we have the term $2(Mc_s - \Delta t K)(\nabla \cdot \tilde{\mathbf{u}}, q)$ bounded as

$$2(Mc_s - \Delta t K)(\nabla \cdot \tilde{\mathbf{u}}, p) = 2(M - \Delta t \frac{K}{c_s})(\nabla \cdot \tilde{\mathbf{u}}, c_s p)$$

$$\geq -\Delta t (M - \Delta t \frac{K}{c_s})\|\nabla \cdot \tilde{\mathbf{u}}\|^2 - \frac{Mc_s^2 - \Delta t c_s K}{\Delta t}\|p\|^2,$$
(36)

which yields

$$\mathcal{L}_{2}(\tilde{\boldsymbol{\sigma}}, \boldsymbol{\eta}) \geq \Delta t^{2} \frac{K}{c_{s}} \|\nabla \cdot \tilde{\mathbf{u}}\|^{2} + \Delta t (1 - \epsilon_{2}) \|\tilde{\mathbf{u}}\|^{2}$$

$$(37) \qquad +c_{s} K \|p\|^{2} + \left(\Delta t K^{2} - \alpha^{2} d C_{PF}^{2} \left(\frac{K^{2}}{\epsilon_{1}} - K\right) \frac{1}{d\lambda + 2\mu}\right) \|\nabla p\|^{2}.$$

If ϵ_1 is chose as $\epsilon_1 = \frac{K}{1 + \frac{\Delta t K (d\lambda + 2\mu)}{2\alpha^2 d C_{PF}^2}} (< K)$,

$$\mathcal{L}_{2}(\tilde{\boldsymbol{\sigma}}, \boldsymbol{\eta}) \geq \Delta t^{2} \frac{K}{c_{s}} \|\nabla \cdot \tilde{\mathbf{u}}\|_{0}^{2} + \Delta t (1 - \epsilon_{2}) \|\tilde{\mathbf{u}}\|^{2}$$

$$+ c_{s} K \|p\|^{2} + \frac{\Delta t K^{2}}{2} \|\nabla p\|^{2},$$
(38)

where ϵ_2 previously chosen for (33) is less than 1. Finally, combining (34) and (33), we have

$$\max\{M, A, K+B\}J_{\Delta t}^{1}(\boldsymbol{\sigma}, \boldsymbol{\eta}, \mathbf{u}, p; \mathbf{0})$$

$$\geq 4KC_{K}\|\nabla \cdot \tilde{\boldsymbol{\sigma}}\|^{2} + (K - \epsilon_{1})\|\mathcal{C}^{-1/2}\tilde{\boldsymbol{\sigma}}\|^{2} + \frac{K}{2}\|\mathcal{C}^{1/2}\varepsilon(\boldsymbol{\eta})\|^{2}$$

$$+\Delta t^{2}\frac{K}{c_{s}}\|\nabla \cdot \tilde{\mathbf{u}}\|^{2} + \Delta t(1 - \epsilon_{2})\|\tilde{\mathbf{u}}\|^{2} + \frac{\Delta t K^{2}}{2}\|\nabla p\|^{2} + c_{s} K\|p\|^{2},$$
(39)

where $\epsilon_1 < K$ and $\epsilon_2 < 1$. Therefore, the first inequality in (BD) follows from (BD). Note that the constant C_1 is independent of Δt . The second inequality is obtained in the standard manner by the triangular inequality and Cauchy-Schwarz inequality. Note that the constant C_2 is dependent on Δt , i.e., $C_2 \sim O(\frac{1}{\Delta t})$.

The upper and lower bounds in (\square) for $\mathcal{J}_{\Delta t}^2$ are shown in a similar manner. All steps are the same as before except for the part to obtain (\square) . The identical

estimate (87) can be obtained for $W_1 = 1$ by proceeding similarly to (85) and (86). Without Δt in the M term we have

$$\mathcal{L}_{2}(\tilde{\boldsymbol{\sigma}}, \boldsymbol{\eta}) \geq M \|\nabla \cdot \tilde{\mathbf{u}}\|^{2} + M \frac{c_{s}^{2}}{(\Delta t)^{2}} \|p\|^{2} + \Delta t (1 - \epsilon_{2}) \|\tilde{\mathbf{u}}\|^{2}$$

$$+ 2(\frac{M}{\Delta t} c_{s} - \Delta t K) (\nabla \cdot \tilde{\mathbf{u}}, p)$$

$$+ \left(\Delta t K^{2} - \alpha^{2} d C_{PF}^{2} \left(\frac{K^{2}}{\epsilon_{1}} - K\right) \frac{1}{d\lambda + 2\mu}\right) \|\nabla p\|^{2}$$

and

$$2(\frac{M}{\Delta t}c_s - \Delta t K)(\nabla \cdot \tilde{\mathbf{u}}, p) = 2(\frac{M}{\Delta t} - \Delta t \frac{K}{c_s})(\nabla \cdot \tilde{\mathbf{u}}, c_s p)$$

$$\geq -\Delta t \left(\frac{M}{\Delta t} - \Delta t \frac{K}{c_s}\right) \|\nabla \cdot \tilde{\mathbf{u}}\|^2 - \frac{(M/\Delta t)c_s^2 - \Delta t c_s K}{\Delta t} \|p\|^2,$$

from which (37) follows.

We now have the following result from Lemma 3.11 and Theorem 3.11. Note that the constant \overline{C} in (27) is dependent on Δt . Thus, the coercivity and continuity properties in the following theorem are valid with the fixed Δt as assumed.

Theorem 3.2. There are positive constants \overline{C}_1 , \overline{C}_2 dependent on Δt satisfying

(40)
$$\overline{C}_1 \| (\boldsymbol{\tau}, \boldsymbol{\xi}, \mathbf{v}, q) \|_{\Delta t}^2 \le J_{\Delta t}^i(\boldsymbol{\tau}, \boldsymbol{\xi}, \mathbf{v}, q; \mathbf{0}) \le \overline{C}_2 \| (\boldsymbol{\tau}, \boldsymbol{\xi}, \mathbf{v}, q) \|_{\Delta t}^2,$$
for $i = 1, 2$ and $\forall (\boldsymbol{\tau}, \boldsymbol{\xi}, \mathbf{v}, q) \in \boldsymbol{\Phi}$.

Remark 3.2. The constant C_1 in (\square) is independent of Δt and $\overline{C} \sim O(\frac{1}{\Delta t})$ in (\square) for a small Δt . Thus, in (\square), $\overline{C}_1 \sim O(\Delta t)$, $\overline{C}_2 \sim O(\frac{1}{\Delta t^2})$ for $J^1_{\Delta t}$ and $\overline{C}_1 \sim O(\Delta t)$, $\overline{C}_2 \sim O(\frac{1}{\Delta t^3})$ for $J^2_{\Delta t}$. However, the difference of how \overline{C}_2 depends on Δt between $J^1_{\Delta t}$ and $J^2_{\Delta t}$ does not affect numerical solutions. It will be demonstrated in Section that both weights in (\square) and (\square) yield equally good numerical solutions.

4. Finite element approximation

For the finite element approximation of (II)-(E), we assume that the domain Ω is a polygon and that \mathcal{T}_h is a collection of finite elements such that $\Omega = \bigcup_{T \in \mathcal{T}_h} T$. Assume that the triangulation \mathcal{T}_h is shape-regular and satisfies the assumption for inverse estimates [5]. For the stress and the fluid velocity in $\mathbf{H}_{div}(\Omega)$ we use the RaviartCThomas elements. Define finite element spaces for the approximate of $(\sigma, \eta, \mathbf{u}, p)$:

(41)
$$\mathbf{S}^h = \{ \boldsymbol{\tau}^h : \boldsymbol{\tau}^h \in \mathbf{S}, \, \boldsymbol{\tau}^h \mid_T \in RT_r(T)^{d \times d} \, \forall T \in \mathcal{T}_h \},$$

(42)
$$\Sigma^h = \{ \boldsymbol{\xi}^h : \boldsymbol{\xi}^h \in \Sigma \cap C^0(\Omega)^d, \, \boldsymbol{\eta}^h \mid_T \in P_{r+1}(T)^d \, \forall T \in \mathcal{T}_h \},$$

(43)
$$\mathbf{X}^h = \{\mathbf{v}^h : \mathbf{v}^h \in \mathbf{X}, \, \mathbf{v}^h \mid_T \in RT_r(T)^d \, \forall T \in \mathcal{T}_h\},$$

$$(44) Q^h = \{q^h \mid q^h \in Q \cap C^0(\Omega), q^h \mid_T \in P_r(T) \ \forall T \in \mathcal{T}_h\},$$

where RT_r , P_r denote the RaviartCThomas element of order r and the piecewise polynomial space of order r, respectively. In the above, the space for η is chosen so that the error estimate for the displacement variable is optimal in a higher norm. The equal order polynomials for η and p will also be considered in numerical experiments. We assume the following standard approximation properties with the interpolation operators \hat{I}_h and \check{I}_h \square , \square :

 $\forall \phi \in H^m(\Omega) \text{ with } \nabla \cdot \phi \in H^m(\Omega) \text{ and }$

(46)
$$\|\varphi - \check{I}_h \varphi\|_l \le \check{C}h^m \|\varphi\|_{m+l} \quad \forall \varphi \in H^{m+l}(\Omega)$$

for $m \leq r+1$ and l=0, 1. Let $\mathbf{\Phi}^h := \mathbf{S}^h \times \mathbf{\Sigma}^h \times \mathbf{X}^h \times Q^h$ be the finite element subspace of $\mathbf{\Phi}$ and consider the discrete least-squares problem for the Biot model: compute $(\boldsymbol{\sigma}^h, \boldsymbol{\eta}^h, \mathbf{u}^h, p^h) \in \mathbf{\Phi}^h$ such that

(47)
$$J_{\Delta t}^{i}(\boldsymbol{\sigma}^{h}, \boldsymbol{\eta}^{h}, \mathbf{u}^{h}, p^{h}; \mathbf{F}) = \inf_{(\boldsymbol{\tau}^{h}, \boldsymbol{\xi}^{h}, \mathbf{v}^{h}, q^{h}) \in \boldsymbol{\Phi}^{h}} J_{\Delta t}^{i}(\boldsymbol{\tau}^{h}, \boldsymbol{\xi}^{h}, \mathbf{v}^{h}, q^{h}; \mathbf{F})$$

for i = 1 or 2.

An a priori error estimate for the primal variables p and η can be derived using Theorem 3.1 and the approximation properties, (45) and (46). First, note from (50) that

$$J_{\Delta t}^{i}(\boldsymbol{\sigma}, \boldsymbol{\eta}, \mathbf{u}, p; \mathbf{0}) \geq C_{1} \left(\|\nabla \cdot \tilde{\boldsymbol{\sigma}}\|^{2} + \|\mathcal{C}^{-1/2} \tilde{\boldsymbol{\sigma}}\|^{2} + \|\mathcal{C}^{1/2} \epsilon(\boldsymbol{\eta})\|^{2} + (\Delta t)^{2} \|\nabla \cdot \tilde{\mathbf{u}}\|^{2} + \Delta t \|\tilde{\mathbf{u}}\|^{2} + \Delta t \|\nabla p\|^{2} + \|p\|^{2} \right)$$

$$(48)$$

for $i=1,\,2$, with C_1 independent of Δt . For the upper bound we only consider $J^1_{\Delta t}$ here. The estimate for $J^2_{\Delta t}$ is obtained by the same way. By Cauchy-Schwarz inequality, $J^1_{\Delta t}$ is bounded above as

$$J_{\Delta t}^{1}(\boldsymbol{\sigma}, \boldsymbol{\eta}, \mathbf{u}, p; \mathbf{0}) \leq \tilde{C}_{2} \left(\|\nabla \cdot \tilde{\boldsymbol{\sigma}}\|^{2} + \|\mathcal{C}^{-1/2} \tilde{\boldsymbol{\sigma}}\|^{2} + \|\mathcal{C}^{1/2} \epsilon(\boldsymbol{\eta})\|^{2} + \frac{1}{\Delta t} \|\boldsymbol{\eta}\|^{2} + \Delta t \|\nabla \cdot \tilde{\mathbf{u}}\|^{2} + \Delta t \|\tilde{\mathbf{u}}\|^{2} + \Delta t \|\nabla p\|^{2} + \frac{1}{\Delta t} \|p\|^{2} \right),$$

$$(49)$$

where C_2 is independent of Δt . Now, (45), (49) and the orthogonality property of $J^1_{\Delta t}$ yield

$$J_{\Delta t}^{1}(\boldsymbol{\sigma}^{h}, \boldsymbol{\eta}^{h}, \mathbf{u}^{h}, p^{h}; \mathbf{F}) = J_{\Delta t}^{1}(\boldsymbol{\sigma} - \boldsymbol{\sigma}^{h}, \boldsymbol{\eta} - \boldsymbol{\eta}^{h}, \mathbf{u} - \mathbf{u}^{h}, p - p^{h}; \mathbf{0})$$

$$\leq J_{\Delta t}^{1}(\boldsymbol{\sigma} - \hat{I}_{h}\boldsymbol{\sigma}, \boldsymbol{\eta} - \check{I}_{h}\boldsymbol{\eta}, \mathbf{u} - \hat{I}_{h}\mathbf{u}, p - \check{I}_{h}\mathbf{p}; \mathbf{0})$$

$$\leq \max\{\hat{C}, \check{C}\} \tilde{C}_{2}h^{2m} \left(\|\nabla \cdot \tilde{\boldsymbol{\sigma}}\|_{m}^{2} + \|\mathcal{C}^{-1/2}\tilde{\boldsymbol{\sigma}}\|_{m}^{2} + \|\mathcal{C}^{1/2}\boldsymbol{\epsilon}(\boldsymbol{\eta})\|_{m}^{2} + \frac{1}{\Delta t} \|\boldsymbol{\eta}\|_{m}^{2} + \Delta t \|\nabla \cdot \tilde{\mathbf{u}}\|_{m}^{2} + \Delta t \|\tilde{\mathbf{u}}\|_{m}^{2} + \Delta t \|\nabla p\|_{m}^{2} + \frac{1}{\Delta t} \|p\|_{m}^{2} \right)$$

$$\leq K_{1}h^{2m} \left(\|\nabla \cdot \boldsymbol{\sigma}\|_{m}^{2} + \|\boldsymbol{\sigma}\|_{m}^{2} + \|\boldsymbol{\eta}\|_{m+1}^{2} + \frac{1}{\Delta t} \|\boldsymbol{\eta}\|_{m}^{2} + \Delta t \|\nabla \cdot \mathbf{u}\|_{m}^{2} + \Delta t \|\mathbf{u}\|_{m}^{2} + \|p\|_{m+1}^{2} + \frac{1}{\Delta t} \|p\|_{m}^{2} \right).$$

$$(50)$$

for some $K_1 > 0$ independent of Δt . Using this estimate and (\square), we get

$$\|\nabla \cdot (\tilde{\boldsymbol{\sigma}} - \tilde{\boldsymbol{\sigma}}^{h})\|^{2} + \|\mathcal{C}^{-1/2}(\tilde{\boldsymbol{\sigma}} - \tilde{\boldsymbol{\sigma}}^{h})\|^{2} + \|\mathcal{C}^{1/2}\epsilon(\boldsymbol{\eta} - \boldsymbol{\eta}^{h})\|^{2} + (\Delta t)^{2} \|\nabla \cdot (\tilde{\mathbf{u}} - \tilde{\mathbf{u}}^{h})\|^{2} + \Delta t \|\tilde{\mathbf{u}} - \tilde{\mathbf{u}}^{h}\|^{2} + \Delta t \|\nabla(p - p^{h})\|^{2} + \|p - p^{h}\|^{2}$$

$$\leq \frac{K_{1}}{C_{1}} h^{2m} \left(\|\nabla \cdot \boldsymbol{\sigma}\|_{m}^{2} + \|\boldsymbol{\sigma}\|_{m}^{2} + \|\boldsymbol{\eta}\|_{m+1}^{2} + \frac{1}{\Delta t} \|\boldsymbol{\eta}\|_{m}^{2} \right)$$

$$+ \Delta t \|\nabla \cdot \mathbf{u}\|_{m}^{2} + \Delta t \|\mathbf{u}\|_{m}^{2} + \|p\|_{m+1}^{2} + \frac{1}{\Delta t} \|p\|_{m}^{2} \right),$$

$$(51)$$

which implies the following estimate for the primal variables:

$$\|\nabla(\boldsymbol{\eta} - \boldsymbol{\eta}^{h})\| + (\Delta t)^{1/2} \|\nabla(p - p^{h})\| + \|p - p^{h}\|$$

$$\leq K_{2}h^{m} \left(\|\nabla \cdot \boldsymbol{\sigma}\|_{m} + \|\boldsymbol{\sigma}\|_{m} + \|\boldsymbol{\eta}\|_{m+1} + \left(\frac{1}{\Delta t}\right)^{1/2} \|\boldsymbol{\eta}\|_{m}\right)$$

$$+ (\Delta t)^{1/2} \|\nabla \cdot \mathbf{u}\|_{m} + (\Delta t)^{1/2} \|\mathbf{u}\|_{m} + \|p\|_{m+1} + \left(\frac{1}{\Delta t}\right)^{1/2} \|p\|_{m}\right),$$
(52)

where $K_2 > 0$ is a constant independent of Δt .

Remark 4.1. If Δt is treated as a fixed constant as assumed, Theorem 3.2 yields the spatial error estimate for all variables: there exists $K_3 > 0$ depends on Δt such that

$$\|\nabla \cdot (\boldsymbol{\sigma} - \boldsymbol{\sigma}^h)\| + \|\nabla (\boldsymbol{\eta} - \boldsymbol{\eta}^h)\| + \|\mathbf{u} - \mathbf{u}^h\|_{H_{div}(\Omega)} + \|\nabla (p - p^h)\|$$

$$\leq K_3 h^m (\|\nabla \cdot \boldsymbol{\sigma}\|_m + \|\boldsymbol{\sigma}\|_m + \|\boldsymbol{\eta}\|_{m+1} + \|\nabla \cdot \mathbf{u}\|_m + \|\mathbf{u}\|_m + \|p\|_{m+1}).$$

5. Numerical implementation

5.1. Test problem 1. The main goal of this test is to compare the accuracy and convergence of WLS finite element solutions, minimizing the functional (ZII) with different weights. We also compare numerical solutions approximated in various combinations of finite element spaces, including nonconforming finite elements spaces for σ and \mathbf{u} . To investigate the convergence of the proposed WLS method, we perform numerical experiments using the non-physical example reported in [III]. Let $\Omega = (0,1) \times (0,1)$ for the domain of model equations. The physical parameters are chosen as $\mu = \alpha = \lambda = K = c_s = 1$. The right-hand side functions f_s , \mathbf{f}_b are chosen so that the exact solution is

$$\mathbf{u} = [-x(\sin(y)e + 2(y-1))e^{-t}, (-\cos(y)e + (y-1)^2)e^{-t}],$$

$$p = (-\sin(y)e + \cos(x)e^y + y^2 - 2y + 1)e^{-t},$$

$$\boldsymbol{\eta} = [\sqrt{2}\cos(\sqrt{2}x)\cos(y)e^{-t}, \sin(\sqrt{2}x)\sin(y)e^{-t}].$$

Conforming finite element spaces were introduced for \mathbf{u} , $\boldsymbol{\sigma}$ in the previous section. However, for the chosen smooth solution above, we also consider nonconforming spaces for those H_{div} functions to compare the performance of the WLS method with or without weights. Since the inf-sup condition is not needed between finite element spaces, P_1 elements for all variables are also used for convenience as tested in 33. We consider four different combinations of finite element spaces for numerical approximations: (P_1, P_1, P_1, P_1) , (RT_1, P_1, P_1, P_1) , (RT_1, P_1, RT_1, P_1) and (RT_1, P_1, RT_1, P_2) for $(\mathbf{u}, p, \sigma, \eta)$ with the refinement step lengths $h = \frac{1}{8}$, $\frac{1}{16}$ and $\frac{1}{32}$. The time step $\Delta t = 0.001$ is chosen for temporal discretization. W_4)=(Δt , 1, Δt , 1). Figures \blacksquare shows errors and convergence rates of the WLS solutions for t = 0.005. We see that the convergence rate for **u** is lower if P_1 is used for the variable **u** instead of RT_1 , while the approximation of σ by P_1 improves errors and convergence. It is also noticeable that the use of P_2 polynomial for η significantly improves the convergence of other variables as well as the convergence of η . Very similar results were obtained with weights (W_1, W_2, W_3, W_4) = $(1, 1, \Delta t, 1)$. Figure 2 compares convergence rates of the LS solutions computed with or without weights on different combinations of finite elements. We observe from Figure 2 that the use of weights does improve the convergence of all variables,

and the optimal orders of accuracy are preserved for the primal variables with either choice of weight combination.

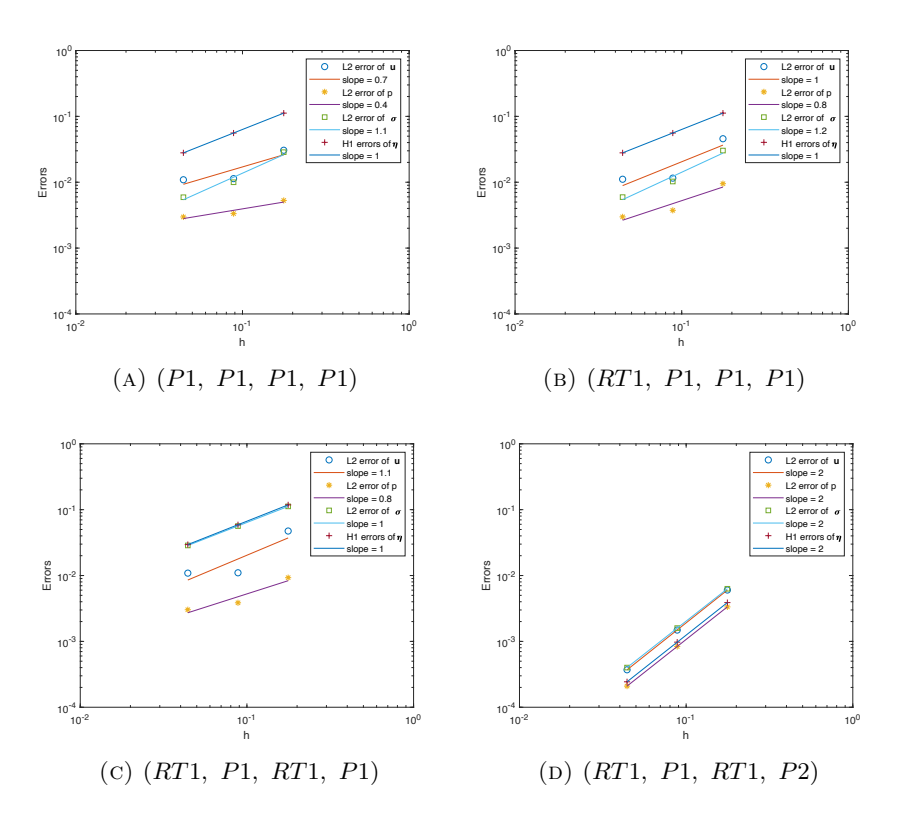


FIGURE 1. Convergence rates of the WLS solutions in different finite element spaces for $(\mathbf{u}, p, \sigma, \eta)$ with $(W_1, W_2, W_3, W_4) = (\Delta t, 1, \Delta t, 1)$ in (\square) .

5.2. Applications in brain intracranial pressure simulation. We apply the WLS method to the benchmark problem reported in [IS], where intracranial pressure (ICP) is simulated using the Biot model. In this brain edema problem, intracranial pressure (ICP) is the growing pressure exerted by fluids or brain swelling inside the skull. The Biot model is reformulated as a three-field system of displacement, total stress, and pressure in their work. The system is then approximated by the Galerkin finite element method with (P_2, P_1, P_1) polynomials, using a coupled or decoupled algorithm.

We conduct numerical simulations based on the physical parameters and boundary conditions used in [IS] and compare simulation results using different weights. The following boundary conditions are considered. On the wall of brain tissue, Γ_1 , the displacement is zero, i.e., $\eta = 0$ on Γ_1 , and $(K\nabla p) \cdot \mathbf{n} = c_b(p_{SAS} - p)$ on Γ_1 , where c_b is the value of conductance and p_{SAS} is the pressure of subarachnoid space of the brain. The balance of flow rate naturally imposes the second condition. On the ventricle wall Γ_2 , the total normal force from the tissue part needs to be balanced with the fluid pressure from the ventricle, that is, $(\boldsymbol{\sigma} - \alpha p) \cdot \mathbf{n} = -p \cdot \mathbf{n}$ on Γ_2 , and the pressure at the ventricle wall is 1100 pa on Γ_2 as in [IS, 27]. The numerical simulation is performed using relevant physical parameters for the brain

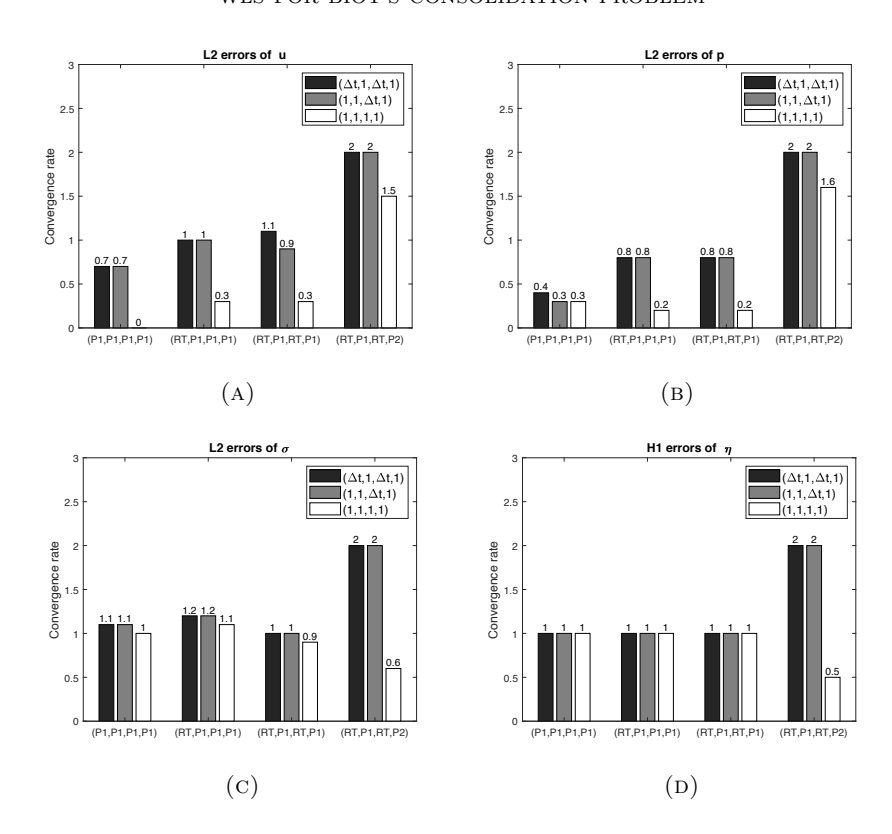


FIGURE 2. Convergence rates of the WLS solutions in different finite element spaces for $(\mathbf{u}, p, \boldsymbol{\sigma}, \boldsymbol{\eta})$: L^2 rates of (\mathbf{a}) \mathbf{u} , (\mathbf{b}) p, (\mathbf{c}) $\boldsymbol{\sigma}$ and (\mathbf{d}) H^1 rates of $\boldsymbol{\eta}$.

Table 1. Parameter values.

Parameters	Values	Parameters	Values
c_s	$4.5 \times 10^{-7} Pa^{-1}$	κ	$1.4 \times 10^{-9} mm^2$
c_b	$3 \times 10^{-5} mm/(Pa \cdot min)$	α	1
p_{SAS}	1070 Pa	ν	0.35
μ_f	$1.48 \times 10^{-5} Pa \cdot min$	E	9010 Pa

model listed in Table Π , and the body force and the source terms are set to zero, i.e., $\mathbf{f}_b = \mathbf{0}$ and $f_s = 0$.

The geometric model presented in Figure \Box (left) is a two-dimensional cross-section of a three-dimensional model generated from the MRI brain atlas \Box After extracting the geometric model, which is 125 mm high and 106 mm wide, we discretize the computation domain by the finite element mesh of 6462 quasi-uniform triangular elements shown in Figure \Box (right). The Biot system is approximated using the element (RT_1, P_1, RT_1, P_1) for $(\mathbf{u}, p, \boldsymbol{\sigma}, \boldsymbol{\eta})$ with the degree of freedom DOF=174477, and the time step $\Delta t = 0.01$. Figure \Box shows the pressure distribution in the brain for t = 0.1 by the WLS method with weights $(W_1, W_2, W_3, W_4) = (\Delta t, 1, \Delta t, 1)$, $(1, 1, \Delta t, 1)$, and (1, 1, 1, 1), and Figure \Box shows its expanded view around the ventricle wall Γ_2 . We see that the pressure profile agrees with that in the normal brain in \Box if the functional $(\Box$) is weighted by



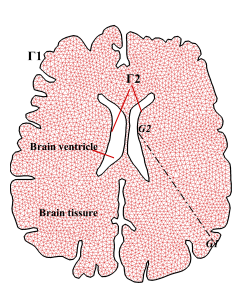


FIGURE 3. An MRI slice of a human brain [32] (left) and its computational domain and FE mesh (right).

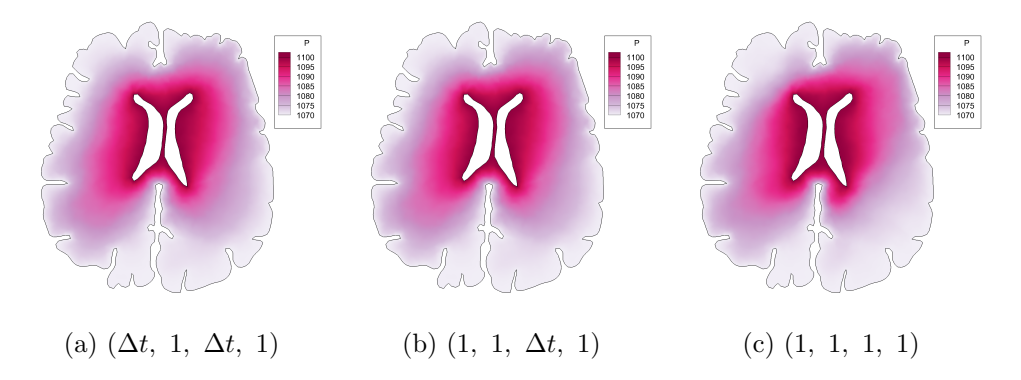


FIGURE 4. Pressure distribution computed by different weights.

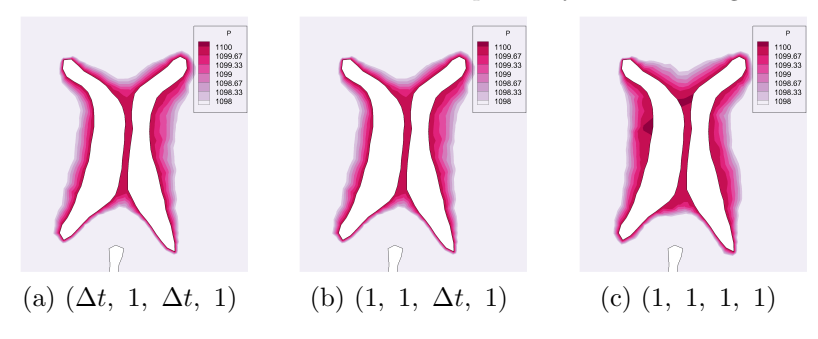


FIGURE 5. Pressure distribution around the ventricle wall Γ_2 .

either $(\Delta t, 1, \Delta t, 1)$ or $(1, 1, \Delta t, 1)$. Also, Figures (a) and (b) show almost identical zoomed-in pressure profiles around the ventricle wall. However, Figure (c) presents higher pressure distribution around the ventricle wall Γ_2 when no weigh is used, i.e., $(W_1, W_2, W_3, W_4) = (1, 1, 1, 1)$. Also, in this case, the lower pressure distribution is observed in the lower right part of the brain in Figure (c). The differences between results in Figure (a)-(c) can be more clearly verified by Figure (b) that presents the pressure along the line segment from G_2 on G_2 to G_1 on G_1 (see Figure (right)). The pressure profiles seem to be in agreement for G_1 on G_2 on G_3 on G_4 on G_4 on G_5 on G_6 on G_7 on G_8 on G_8 on G_9 on

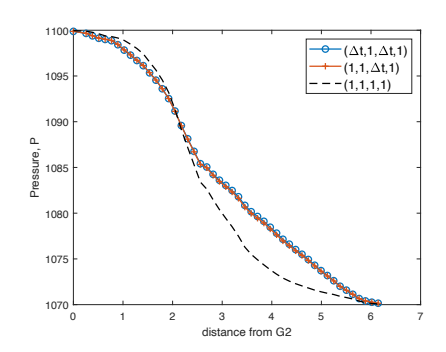


FIGURE 6. Plots of pressure along the line segment from G_2 to G_1 .

6. Conclusion

We studied a WLS finite element method for the full quasi-static model with all modeling parameters. The WLS functional was defined by the L^2 residuals of temporal discretized equations and weighted by the time step. The WLS functional was analyzed for coercivity and continuous properties, and an error estimate was derived for the primal solution variables approximated in conforming finite element spaces. For numerical experiments, we first considered a non-physical example to illustrate our theoretical results. For the non-physical problem, we observed that the WLS solutions exhibit the optimal convergence rates. Finally, we extended the implementation of this method to a benchmark problem for brain pressure simulations $[\mathbb{R}]$. The WLS solution agreed with the published work, which further validates the effectiveness of our approach.

Acknowledgments

H.-C. Lee's work was partially supported by the Taiwan MOST grant 109-2115-M-160-001. H. Lee's work was partially supported by the NSF under grant number DMS-1818842.

References

- S. Bidwell, M. E. Hassell and C. R. Westphal, A weighted least-squares finite element method for elliptic problems with degenerate and singular coefficients, Math. Comp. 82, 2013, pp. 673-688.
- M. A. Biot, General theory of three-dimensional consolidation, J. Appl. Phys. 12, 1941, pp. 155-164.
- [3] M. A. Biot, General solutions of the equations of elasticity and consolidation of a porous material, J. Appl. Phys. 23, 1956, pp. 91-96.
- [4] P. B. Bochev and M. D. Gunzburger, Analysis of least-squares finite element methods for the Stokes equations, Math. Comput. 6, 1994, pp. 479C506.
- [5] S. C. Brenner and L. R. Scott, The Mathematical Theory of Finite Element Methods, Springer, New York, 2002.
- [6] F. Brezzi and M. Fortin, Mixed and Hybrid Finite Element Methods, Springer, New York, 1991.
- [7] Z. Cai, J. Korsawe and G. Starke, An adaptive least-squares mixed finite element method for the stress-displacement formulation of linear elasticity, Numer. Methods Partial Differ. Equ. 21, 2005, pp. 132-148.
- [8] Z. Cai and G. Starke, First-order system least-squares for the stress-displacement formulation: Linear elasticity, SIAM J. Numer. Anal. 41, 2003, pp. 715-730.
- [9] Z. Cai and G. Starke, Least-squares methods for linear elasticity, SIAM J. Numer. Anal. 42, 2004, pp. 826-842.

- [10] Z. Cai and C. R. Westphal, A weighted H(div) least-squares method for second-order elliptic problems, SIAM J. Numer. Anal. 40, 2008, pp. 1640C1651.
- [11] A. Cesmelioglu, H. Lee, A. Quaini, K. Wang and S. Y. Yi, Optimization-based decoupling algorithms for a fluid-poroelastic system, S.C. Brenner (ed.), Topics in Numerical Partial Differential Equations and Scientific Computing, The IMA Volumes in Mathematics and its Applications 160, 2016, pp. 79-98.
- [12] T. F. Chen, C. L. Cox, H. C. Lee and K. L. Tung, Least-squares finite element methods for generalized Newtonian and viscoelastic flows, Appl. Numer. Math. 60, 2010, pp. 1024-1040.
- [13] Y. Chen, Y. Luo and M. Feng, Analysis of a discontinuous Galerkin method for the Biots consolidation problem, Appl. Math. Comput. 219, 2013, pp. 9043-9056.
- [14] X. Feng, Z. Ge and Y. Li, Analysis of a multiphysics finite element method for a poroelasticity model, IMA Journal of Numerical Analysis 38, 2018, pp. 330C359.
- [15] M. Ferronato, N. Castelletto and G. Gambolati, A fully coupled 3-d mixed finite element model of Biot consolidation, J. Comput. Phys. 229, 2010, pp. 4813-4830.
- [16] F. J. Gaspar, F. J. Lisbona and P. N. Vabishchevich, A finite difference analysis of Biots consolidation model, Appl. Numer. Math. 44, 2003, pp. 487-506.
- [17] J. B. Haga, H. Osnes and H. P. Langtangen, On the causes of pressure oscillations in low-permeable and low-compressible porous media, Int. J. Numer. Anal. Methods Geomech. 36, 2012, pp.1507-1522.
- [18] G. Ju, M. Cai, J. Li and J. Tiand, Parameter-robust multiphysics algorithms for Biot model with application in brain edema simulation, Math. Comput. Simulat. 177, 2020, pp. 385-403.
- [19] G. Kanschat and B. Riviere, A finite element method with strong mass conservation for Biots linear consolidation model, J. Sci. Comput. 77, 2018, pp. 1762-1779.
- [20] J. Korsawe and G. Starke, A least-squares mixed finite element method for Biot's consolidation problem in porous media, SIAM J. Numer. Anal. 43, 2005, pp. 318-339.
- [21] J. Korsawe, G. Starke, W. Wang and O. Kolditz, Finite element analysis of poro-elastic consolidation in porous media: Standard and mixed approaches, Comput. Methods. Appl. Mech. Engrg. 195, 2006, pp. 1096-1115.
- [22] J. Kraus, P. L. Lederer, M. Lymbery and J. Schöberlb, Uniformly well-posed hybridized discontinuous Galerkin/hybrid mixed discretizations for Biots consolidation model, Comput. Methods. Appl. Mech. Engrg. 384, 2021, DOI:10.1016/j.cma.2021.113991.
- [23] E. Lee, T. A. Manteuffel and C. R. Westphal, Weighted-norm first-order system least-squares (FOALS) for Problems with Corner Singularities, SIAM J. Numer. Anal. 44, 2006, pp. 1974C1996.
- [24] H. C. Lee, and T. F. Chen, A nonlinear weighted least-squares finite element method for Stokes equations, Comput. Math. with Appl. 59, 2010, pp. 215-224.
- [25] H. C. Lee, A nonlinear weighted least-squares finite element method for the Oldroyd-B viscoelastic flow, Appl. Math. Comput. 219, 2012, pp. 421-434.
- [26] J. J. Lee, Robust error analysis of coupled mixed methods for Biots consolidation model, J. Sci. Comput. 69, 2016, pp. 610C632.
- [27] X. Li, H. V. Holst and S. Kleiven, Influence of gravity for optimal head positions in the treatment of head injury patients, Acta Neurochirurgica volume 153, 2011, pp. 2057C2064.
- [28] M. A. Murad, V. Thomée, and A. F. D. Loula, Asymptotic behavior of semidiscrete finiteelement approximations of Biots consolidation problem, SIAM J. Numer. Anal. 33, 1996, pp. 1065C1083.
- [29] P. J. Phillips and M. F. Wheeler, A coupling of mixed and continuous Galerkin finite element methods for poroelasticity I: the continuous in time case, Comput. Geosci. 11, 2007, pp. 131C144.
- [30] P. J. Phillips and M. F. Wheeler, Overcoming the problem of locking in linear elasticity and poroelasticity: an heuristic approach, Comput. Geosci. 13, 2009, pp. 5C12.
- [31] W. Qi, P. Seshaiyer and J. Wang, Finite element method with the total stress variable for Biot's consolidation model, Numer. Methods Partial Differ. Equ., 2021, doi.org/10.1002/num.2272.
- [32] R. E. Showalter and T. W. Ting, Pseudoparabolic partial differential equations, SIAM J. Math. Anal. 1, 1970, pp. 1-26.
- [33] M. Tchonkova, J. Peters and S. Sture, A new mixed finite element method for poro-elasticity, Int. J. Numer. Anal. Methods Geomech. 32, 2008, pp. 579-606.
- [34] S. Y. Yi, A coupling of nonconforming and mixed finite element methods for Biots consolidation model, Numer. Methods Partial Differ. Equ. 29, 2013, pp. 1749-1777.

- [35] S. Y. Yi, Convergence analysis of a new mixed finite element method for Biots Consolidation Model, Numer. Methods Partial Differ. Equ. 30, 2014, pp. 189-1210.
- [36] A. Zenisek, The existence and uniqueness theorem in Biots consolidation theory, Applied Math. 29, 1984, pp. 194-211.
- [37] http://www.med.harvard.edu/aanlib/cases/caseNA/pb9.htm.

Center for General Education, Wenzao Ursuline University of Languages, 900 Mintsu 1st Road Kaohsiung, Taiwan

E-mail: 87013@mail.wzu.edu.tw

School of Mathematical and Statistical Sciences, Clemson University, Clemson, SC 29634-0975

 $E ext{-}mail: \ \mathtt{hklee@clemson.edu}$